Imino Sugars Are Potent Agonists of the Human Glucose Sensor SGLT3

Andrew A. Voss, Ana Díez-Sampedro, Bruce A. Hirayama, Donald D. F. Loo, and Ernest M. Wright

Department of Physiology, David Geffen School of Medicine at University of California Los Angeles, Los Angeles, California

Received August 25, 2006; accepted November 15, 2006

ABSTRACT

Imino sugars are used to treat type 2 diabetes mellitus [miglitol (Glyset)] and lysosomal storage disorders [miglustat (Zavesca)] based on the inhibition of α-glucosidases and glucosyltransferases. In this substrate specificity study, we examined the interactions of imino sugars with a novel human glucose sensor, sodium/glucose cotransporter type 3 (hSGLT3), using expression in *Xenopus laevis* oocytes and electrophysiology. The results for hSGLT3 are compared with those for α-glucosidases and human SGLT type 1 (hSGLT1), a well characterized sodium/glucose cotransporter of the SGLT family. In general, substrates have lower apparent affinities ($K_{0.5}$) for hSGLT3 than hSGLT1 (D-glucose, α-methyl-D-glucose, 1-deoxy-D-glucose, and 4-deoxy-4-fluoro-D-glucose exhibit $K_{0.5}$ values of 19, 21, 43, and 17 mM, respectively, for hSGLT3, and 0.5, 0.7, 10, and 0.07 mM, respectively, for hSGLT1). However, specificity of hSGLT3 binding is greater (D-galactose and 4-deoxy-4-fluoro-D-galactose are not hSGLT3 substrates, but have hSGLT1 $K_{0.5}$ values of 0.6 and 1.3 mM). An important deviation from this trend is potent hSGLT3 activation by the imino sugars 1-deoxynojirimycin (DNJ), *N*-hydroxylethyl-1-deoxynojirimycin (miglitol), *N*-butyl-1-deoxynojirimycin (miglustat), *N*-ethyl-1-deoxynojirimycin, and 1-deoxynojirimycin-1-sulfonic acid, with $K_{0.5}$ values of 0.5 to 9 μM. The diastereomer 1-deoxygalactonojirimycin activates hSGT3 with a $K_{0.5}$ value of 11 mM, a 3000-fold less potent interaction than is observed for DNJ (4 μM). These imino sugar binding characteristics are similar to those for α-glucosidases, but there are no interactions with hSGLT1. This work provides insights into hSGLT3 and -1 substrate binding interactions, establishes a pharmacological profile to study endogenous hSGLT3, and may have important ramifications for the clinical application of imino sugars.

Efforts to curb the emerging epidemics of diabetes and obesity are focusing on dietary supplements for prevention and treatment. Important therapeutics emerging from these efforts are imino sugars. For example, *N*-hydroxylethyl-1-deoxynojirimycin [miglitol (Glyset)] is used to treat type 2 diabetes mellitus based on α-glucosidase inhibition (For meta-analysis, see van de Laar et al., 2005). In the gastrointestinal (GI) tract, α-glucosidases convert disaccharides to monosaccharides, which is necessary for absorption. Inhibition of α-glucosidases by miglitol hence reduces intestinal glucose absorption and, subsequently, blood glucose levels.

Beyond the GI tract, the imino sugar *N*-butyl-1-deoxynojirimycin [miglustat (Zavesca)] is used to treat lysosomal storage disorders based on glucosyltransferase inhibition (Butters et al., 2005). Our attention was drawn to imino sugars based on their GI activity, because we recently identified a novel human glucose sensor, the sodium/glucose cotransporter type 3 (hSGLT3) expressed in the GI tract and neuromuscular junction of skeletal muscle (Díez-Sampedro et al., 2003; Wright et al., 2006).

hSGLT3 is 1 of 11 members of the functionally diverse human *SLC5* gene family (Wright et al., 2004; Wright et al., 2006). In the presence of D-glucose (glucose), hSGLT3 depolarizes the membrane potential because of an uncoupled inward Na$^+$ current at pH 7.5 (Díez-Sampedro et al., 2003), mediated by a transporter and/or channel mechanism. This glucose-activated inward Na$^+$ current is not accompanied by

ABBREVIATIONS: GI, gastrointestinal; hSGLT3, human sodium/glucose cotransporter type 3; hSGLT1, human sodium/glucose cotransporter type 1; αMDG, α-methyl-D-glucose; E_m, membrane potential; $\Delta E_{m(max)}$, maximum change in membrane potential; I_{max}, maximal current; glucose, D-glucose; galactose, D-galactose; 1DOglc, 1-deoxy-D-glucose (1,5-anhydro-D-glucitol); 2DOglc, 2-deoxy-D-glucose; 3DOglc, 3-deoxy-D-glucose; 4DOglc, 4-deoxy-D-glucose ; 4D4Fglc, 4-deoxy-4-fluoro-D-glucose; 4D4Fgal, 4-deoxy-4-fluoro-D-galactose; DNJ, 1-deoxynojirimyin; DGJ, 1-deoxygalactonojirimycin; NE-DNJ, *N*-ethyl-1-deoxynojirimycin; 1SO-DNJ, 1-deoxynojirimycin-1-sulfonic acid; NEOH-DNJ, *N*-β-hydroxyethyl-1-deoxynojirimycin (miglitol); NB-DNJ, *N*-butyl-1-deoxynojirimycin (miglustat).

glucose transport, unlike other members of the *SLC5* gene family. For example, hSGLT1, the best characterized member of this family, actively cotransports Na^+ and glucose in a tight 2:1 stoichiometry (Parent et al., 1992a,b; Mackenzie et al., 1998). Supporting the glucose-sensing role for hSGLT3 is its expression in the intestinal autonomic nervous system and neuroendocrine cells of the GI tract, where there is evidence that hSGLT3 substrates stimulate peptide and 5-hydroxytryptamine secretion (Freeman et al., 2006; Wright et al., 2006).

In this study, we examine the hSGLT3 substrate specificity, including interactions with imino sugars, and compare the results with those for hSGLT1 and α-glucosidases. The experiments were performed using electrophysiological assays on *X. laevis* oocytes expressing hSGLT3 or hSGLT1. Two of the imino sugars examined are miglitol and miglustat. The results are discussed in terms of the molecular architecture of the substrate binding site. We find that imino sugars are potent and specific agonists of hSGLT3 but not hSGLT1. In contrast, hSGLT3 exhibits substrate specificity similar to α-glucosidases, suggesting an analogous substrate binding site. Hence, a crystal structure of a α-glucosidase with bound imino sugar is used to provide clues into the architecture of the hSGLT3 binding site. Potential physiological ramifications of clinically used imino sugars targeting hSGLT3 glucose sensors are discussed.

Materials and Methods

Materials. Substrates were purchased from Sigma (St. Louis, MO), Toronto Research Chemicals (North York, ON, Canada), or CMS Chemicals (Oxfordshire, UK). All other chemicals were purchased from Sigma or Fisher Chemicals (Fairlawn, NJ).

Expression of Human SGLT3 and 1 in *Xenopus laevis* Oocytes. Stage V–VI oocytes were extracted from *X. laevis* (NASCO, Fort Atkinson, WI) ovaries as approved by the University of California Chancellor's Committee on Animal Research (Ikeda et al., 1989; Parent et al., 1992a). Oocytes were isolated from ovaries using 3 mg/ml collagenase type 1 in Barth's solution (Parent et al., 1992a) for 1 h and defolliculated with 0.02 g/ml bovine serum albumin and 120 mM KH_2PO_4 for 30 min. Oocytes were then injected with 50 ng of hSGLT3 (Diez-Sampedro et al., 2003) or hSGLT1 (Hediger et al., 1989) cRNA and maintained at 18°C for 3 to 6 days before use in Barth's solution with 5 mg/ml gentamycin, 5.75 mg/ml ciprofloxacin (Bayer, West Haven, CT), and 100 units/ml penicillin G sodium–100 mg/l streptomycin sulfate (Invitrogen, Carlsbad, CA).

Electrophysiology. cRNA-injected and control noninjected oocytes were impaled with two microelectrodes, each filled with 3 M KCl and having a resistance of 0.5 MΩ, in a rapid perfusion chamber (Parent et al., 1992a; Loo et al., 1993). Oocytes were superfused at 22°C and exposed to sugars dissolved in a Na^+ buffer (100 mM NaCl, 2 mM KCl, 1 mM $MgCl_2$, 1 mM $CaCl_2$, and 10 mM HEPES/Tris, pH 7.4). Na^+-free conditions were achieved by substituting choline for Na^+. Steady-state changes in membrane potential and current were measured under open-circuit conditions and voltage-clamp at -50 mV, respectively. Voltage-clamp experiments were controlled with CLAMPEX in pCLAMP (Molecular Devices, Sunnyvale, CA) and continuous recordings of membrane potential and current were acquired with a chart recorder.

Under open circuit conditions, apparent affinities ($K_{0.5}$) and maximal substrate-induced membrane potential changes [$\Delta E_{m(max)}$] were calculated with the equation $\Delta E_m / \Delta E_{m(max)} = [S]/(K_{0.5} + [S])$, with [S] = sugar concentration. Likewise, under voltage-clamp conditions, apparent affinities ($K_{0.5}$) and maximal substrate-induced currents (I_{max}) are calculated using $I/I_{max} = [S]/(K_{0.5} + [S])$. Student's *t* tests

and estimations of kinetic parameters are presented as mean values $\pm$ S.D. (*n* = number of observations), and curve-fittings using the nonlinear and linear fitting methods were derived with SigmaPlot (Systat Software, Point Richmond, CA).

Inhibition of hSGLT3 by phlorizin was assessed via Dixon plots, with inhibition of sugar-induced depolarizations measured at 10, 20, and 40 mM α-methyl-D-glucose (αMDG). For each αMDG concentration, the reciprocal of the inhibited depolarization induced by phlorizin was analyzed by linear regression. The inhibition constant (K_i) was the negative inhibition concentration where the regression lines intersected.

Results

The proposed physiological role of hSGLT3 is depolarization of the resting membrane potential in response to external glucose. Thus, membrane depolarizations measured under open-circuit conditions were used predominantly to monitor hSGLT3 responses to various agonists or antagonists (Fig. 1 shows representative structures). αMDG was chosen as the model substrate because it is specific for SGLTs relative to the GLUT facilitative sugar transporters (Wright et al., 1980; Díez-Sampedro et al., 2001) and is not metabolized. The maximum depolarizations observed for αMDG ranged between 5 and 20 mV, depending on the hSGLT3 expression level. To account for variable expression levels, the kinetics presented in this study were normalized with respect to the maximal αMDG-induced depolarization measured in the same oocyte.

hSGLT3 Kinetics for Glucose and αMDG. The time course of the resting membrane potential (E_m) of an oocyte injected with hSGLT3-cRNA and bathed in a Na^+ buffer is shown in Fig. 2A. Addition of 20 mM αMDG resulted in a 5-mV depolarization that was fully reversible. Subsequent exposure to 20 mM glucose also induced a reversible 5-mV depolarization. Figure 2B illustrates that the hSGLT3 re-
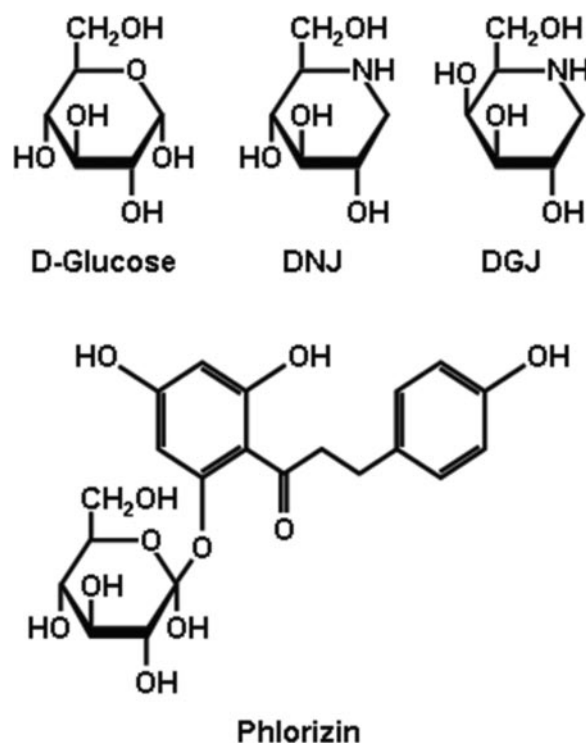

Fig. 1. Chemical structures of glucose, DNJ, DGJ, and phlorizin.

sponses to αMDG and glucose in this oocyte had similar apparent affinities ($K_{0.5}$) and maximum depolarizations [$\Delta E_{m(max)}$]. Experiments with additional oocytes demonstrated that the $K_{0.5}$ values for αMDG and glucose of 21 $\pm$ 6 mM ($n = 42$) and 19 $\pm$ 6 mM ($n = 3$), respectively, were not significantly different ($p > 0.5$). The kinetics of hSGLT3 activation by αMDG were also measured under voltage-clamp (-50 mV). The $K_{0.5}$ value was 22 $\pm$ 3 mM ($n = 3$), which was not significantly different from the aforementioned $K_{0.5}$ derived under open-circuit conditions ($p > 0.5$).

Sugar Selectivity. For hSGLT3, the role of the glucose hydroxyl at carbon number 1 (C1-OH) was assessed by measuring the depolarizations induced by 0 to 100 mM 1,5-anhydro-D-glucitol (1-deoxy-D-glucose, 1DOglc). This resulted in a $K_{0.5}$ = 43 $\pm$ 10 mM and $\Delta E_{m(max)}$ relative to 100 mM αMDG of 170 $\pm$ 20%, $n = 4$ (Fig. 3). The same approach was used to assess the C2- and C3-OH moieties. Exposure to 2-deoxy-D-glucose (2DOglc) or 3-deoxy-D-glucose (3DOglc) induced no observable changes in E_m at concentrations up to 100 mM. Neither 2DOglc (50 mM) nor 3DOglc (20 mM) inhibited depolarizations induced by 5 or 10 mM αMDG. Analysis of the C4-OH with 4-deoxy-D-glucose (4DOglc) resulted in a $K_{0.5} > 50$ mM and $\Delta E_{m(max)}$ that was not deter-minable at concentrations up to 100 mM. For the C6-OH, exposure to 0 to 100 mM 6-deoxy-D-glucose resulted in small depolarizations that precluded an accurate analysis. We estimated the $K_{0.5} > 50$ mM. To extend this study to hitherto untested aspects of hSGLT1, we exposed oocytes expressing hSGLT1 and voltage-clamped at -50 mV to 10 mM 3DOglc and observed no inhibitory effect on the steady-state currents induced by 1 mM αMDG. Exposure to 0 to 5 mM 4DOglc ($n = 3$) under voltage-clamp (-50 mV) resulted in activation with a $K_{0.5} = 0.4 \pm 0.05$ mM and $I_{max} = 100 \pm 3\%$ of αMDG.

Because hSGLT3 discriminates between glucose and D-galactose (galactose) (Díez-Sampedro et al., 2003), diastereomers at the C4-OH, this hydroxyl group was examined further. To verify that galactose does not interact with hSGLT3, we tested for inhibition and observed that 20 mM galactose had no detectable effect on depolarizations induced by 5 mM αMDG. The interaction of the C4-OH with hSGTL3 was also assessed with fluorine substitution. Exposing hSGLT3 to 4-deoxy-4-fluoro-D-glucose (4D4Fglc) resulted in activation with a $K_{0.5} = 17 \pm 1$ mM and $\Delta E_{m(max)} = 100 \pm 4\%$ of αMDG ($n = 3$), neither of which was statistically different from αMDG ($p > 0.2$; Fig. 3). In contrast, 50 mM 4-deoxy-4-fluoro-D-galactose (4D4Fgal) had no effect on the E_m and 20 mM 4D4Fgal failed to inhibit depolarizations induced by 5 mM αMDG. In extending these fluorine substitution studies to hitherto-untested aspects of hSGLT1, exposure to 4D4Fgal ($n = 3$) resulted in a $K_{0.5} = 1.3 \pm 0.1$ mM and $I_{max} = 110 \pm 2\%$ of αMDG.

Inhibition of hSGLT3. Phlorizin (Fig. 1), a high-affinity hSGLT1 competitive inhibitor, also inhibited hSGLT3. The inhibition constant (K_i) was determined by measuring the inhibitory effect of 0.010 to 1.0 mM phlorizin on depolarizations induced by 10 to 40 mM αMDG. Plotting the reciprocal of these responses as a function of phlorizin concentration (Dixon plot) in three experiments yields a $K_i = 0.12 \pm 0.05$ mM (Fig. 4). In the absence of an activating sugar, 1 mM phlorizin induced a hyperpolarization of ~2 mV, depending on the hSGLT3 expression level. In control noninjected oocytes, 1 mM phlorizin did not induce a detectable response, which suggests that phlorizin blocks a sugar-independent inward current mediated by hSGLT3, as occurs with hSGLT1 (Parent et al., 1992a,b).

Effects of Imino Sugars. The contribution of the pyranose oxygen was examined by measuring the responses to a series of imino sugars based on 1-deoxynojirimyin (DNJ; Fig. 1). Exposure of hSGLT3 to DNJ revealed potent activation
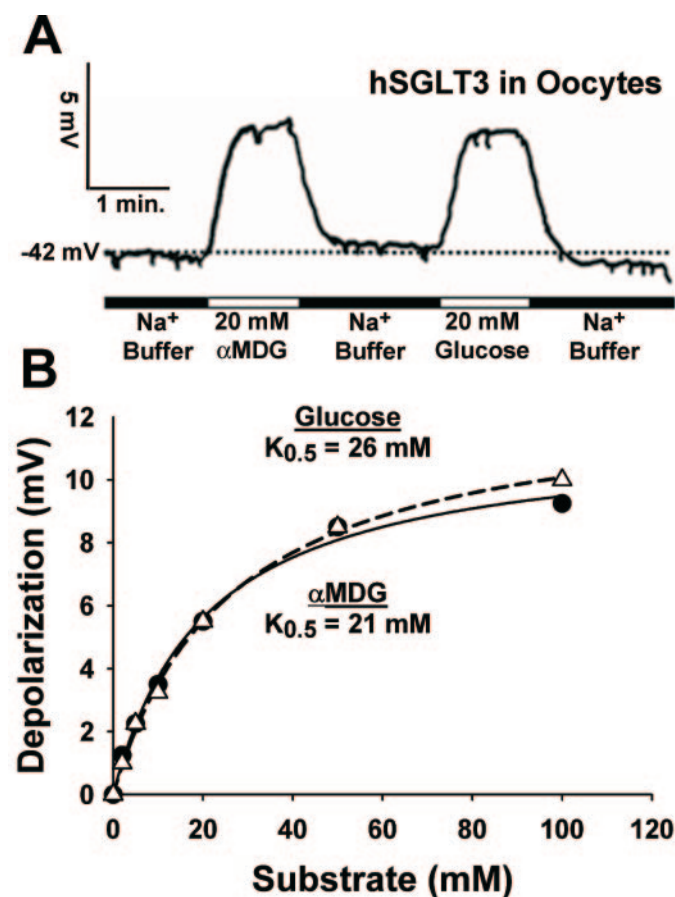
Fig. 2. hSGLT3 in *X. laevis* oocytes. A, a time course of the resting membrane potential from an oocyte expressing hSGLT3 illustrating analogous 5 mV membrane depolarizations (upward deflections) induced by 20 mM αMDG and glucose. The oocyte was under constant perfusion and the sugars were dissolved in Na$^+$ buffer (see *Materials and Methods*). The resting membrane potential was -42 mV. B, from the same hSGLT3 oocyte, a representative plot of the membrane depolarizations induced by 0 to 100 mM αMDG and glucose. The dose-response relations were fitted with Michaelis-Menten kinetics (see *Materials and Methods*).
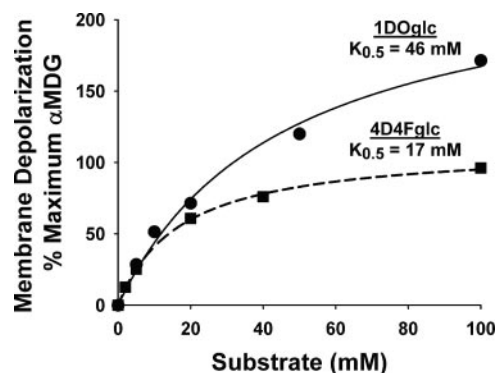
Fig. 3. Activation of hSGLT3 by deoxy-glucose analogs. Representative dose-response curves of hSGLT3 activation by 0 to 100 mM 1DOglc and 4D4Fglc. The curves were normalized to the maximum depolarization observed for αMDG (100 mM) from the same oocyte.

with a $K_{0.5} = 4 \pm 1$ μM (Fig. 5, A and B). To test for stereospecificity in the imino sugars as observed with glucose and galactose, hSGLT3 was exposed to 1-deoxygalactonojirimycin (DGJ) (Fig. 1), which resulted in a substantially less potent activation relative to DNJ, with a $K_{0.5} = 11 \pm 4$ mM (Fig. 5A). To examine the affect of N-alkylation and substitution at C1 of DNJ, hSGLT3 was exposed to N-ethyl-1-deoxynojirimycin (NE-DNJ) and 1-deoxynojirimycin-1-sulfonic acid (1SO-DNJ), which also resulted in potent activation with $K_{0.5}$ values = 3 ± 1 and 9 ± 4 μM (Fig. 5B). The effect of N-alkylation was further tested with the clinically administered N-β-hydroxyethyl-1-deoxynojirmycin (miglitol, NEOH-DNJ) and N-butyl-1-deoxynojirimycin (miglustat, NB-DNJ), which resulted in activation with $K_{0.5}$ values = 3 ± 1 and 0.5 ± 0.1 μM, respectively (Fig. 5C).

In addition, greater maximal responses relative to αMDG were observed for DGJ, DNJ, and NEOH-DNJ with $\Delta E_{\mathrm{m(max)}}$ values = 440 ± 74, 260 ± 36, and $200 \pm 22\%$ that of αMDG, respectively (Fig. 5, A and C). The $\Delta E_{\mathrm{m(max)}}$ values for NE-DNJ, 1SO-DNJ, and NB-DNJ of 130 ± 36, 100 ± 30, and $88 \pm 11\%$ of αMDG, respectively, were not significantly different from αMDG ($p > 0.2$, Fig. 5, B and C). The activation of hSGLT3 by imino sugars was also studied under voltage clamp. At -50 mV, the maximal inward current induced by DNJ (250 μM) was 55 nA, compared with the 19 nA induced by αMDG (100 mM) in the same oocyte. Thus, the ratio of the maximal current induced by DNJ and αMDG was similar (290%) to the membrane depolarizations induced by the sugars.

The depolarizations induced by hSGLT3 in response to imino sugars were tested for phlorizin sensitivity. In the presence of 1 mM phlorizin, the depolarizations induced by 2 μM DNJ, NEOH-DNJ, NE-DNJ, and 1SO-DNJ were inhibited by 80, 80, 70, and 90%; 0.5 μM NB-DNJ was inhibited by 80%. The effect of imino sugars on hSGLT3 was Na$^+$-dependent; in the absence of Na$^+$, 25 μM DNJ and 20 μM NEOH-DNJ induced no observable change in E_{m} (data not shown).

For hSGLT1, in contrast, no observable responses were induced by exposure to 20 mM DNJ, 5 mM DGJ, 50 μM NEOH-DNJ, NE-DNJ, and 1SO-DNJ, and 20 μM NB-DNJ. Likewise, no observable responses were detected in control noninjected oocytes.

Discussion

This study identifies specific agonists needed to elucidate the physiological role of the putative glucose sensor hSGLT3
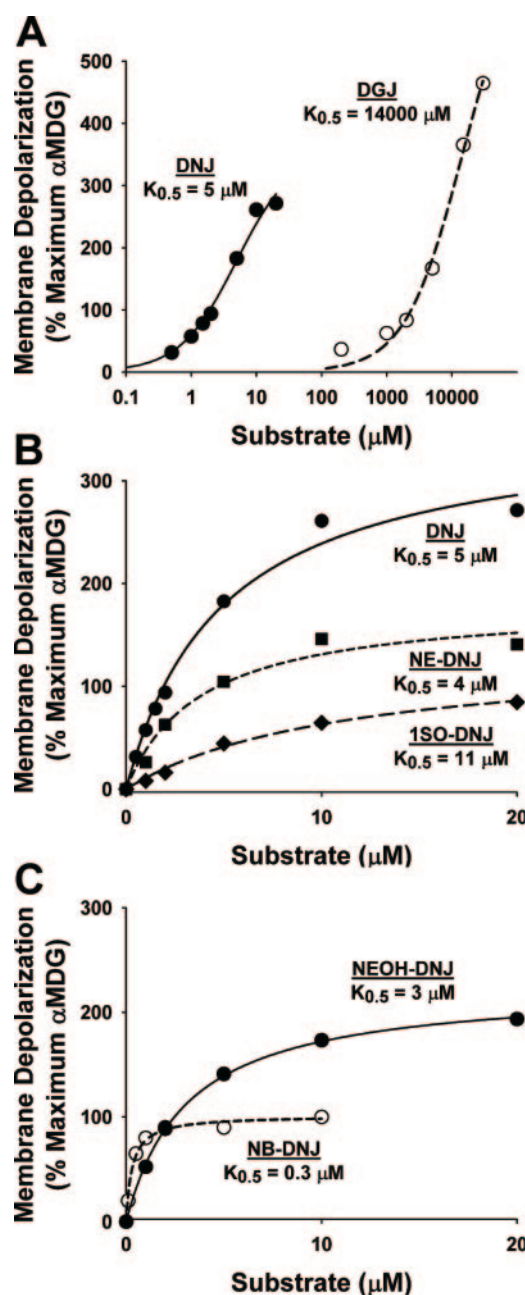
Fig. 5. Activation of hSGLT3 by imino sugars. The typical membrane depolarizations induced by hSGLT3 in response to: A, 0.5 to 20 μM DNJ and 200 to 30,000 μM DGJ (a logarithmic scale was used for the large concentration range); B, 0 to 20 μM DNJ, NE-DNJ, and 1SO-DNJ; and C, 0 to 20 μM NEOH-DNJ (miglitol) and 0 to 10 mM NB-DNJ (miglustat). Each response was normalized to the maximum depolarization observed for αMDG (100 mM) from the same oocyte.
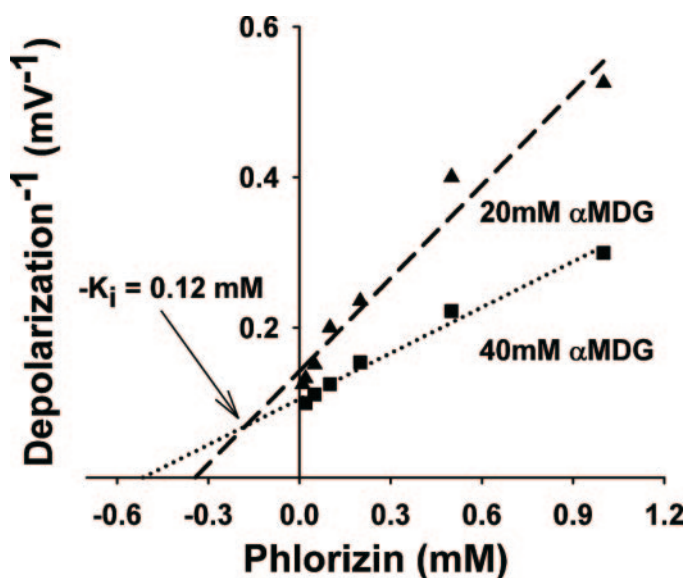

Fig. 4. Inhibition of hSGLT3 by phlorizin. A Dixon plot illustrating the ability of phlorizin (0.010–1.0 mM) to inhibit hSGLT3 responses (membrane depolarizations) to 20 and 40 mM αMDG. The reciprocals of the depolarizations measured for each αMDG concentration were plotted as a function of phlorizin concentration. A linear regression of the responses from each αMDG concentration was generated and the inhibition constant (K_{i}) was derived from the points of intersection (see *Materials and Methods*). The K_{i} value presented is the average value obtained from three different experiments.

(Diez-Sampedro et al., 2003). We employ *X. laevis* oocyte expression and an electrophysiological assay to compare the substrate specificity of hSGLT3 relative to hSGLT1. The affinity and efficacy of deoxy- and imino-sugars are measured relative to those for a nonmetabolized model substrate, αMDG. In general, hSGLT3 substrate binding occurs with lower affinity but greater specificity compared with hSGLT1 (Table 1). For example, the hSGLT3 apparent affinity for glucose is 40-fold lower that of hSGLT1, and hSGLT3 does not recognize galactose, whereas hSGLT1 indiscriminately transports both glucose and galactose. A striking exception to this pattern is a very high hSGLT3 affinity for imino sugars (glucose $K_{0.5}$/NB-DNJ $K_{0.5}$ = 40,000), which are not recognized by hSGLT1 (Table 1). This indicates that imino sugars are excellent substrates to determine the physiological role of hSGLT3. To the best of our knowledge, this is the first report revealing that imino sugars target hSGLT3, which may have important ramifications for the clinical application of imino sugars.

Comparison with α-Glucosidases. Several aspects of hSGLT3 substrate selectivity (Table 1) are similar to those identified for α-glucosidases (Platt and Butters, 2000; Asano, 2003). For example: 1) the affinity range for imino sugars—maltase exhibits IC_{50} values of 0.36 μM for DNJ to 2.1 μM for NB-DNJ to infinity for DGJ (Godin et al., 2004; Kato et al., 2005); 2) there is at least a 1000-fold higher affinity for imino sugars than for endogenous sugars; 3) *N*-alkylation of imino sugars is well tolerated; 4) the glucose C2-, 3-, 4-, and 6-OH groups are required for high-affinity binding; and 5) the C1-OH is not required for binding. Some differences also exist, reflected by the higher hSGLT3 apparent affinity for NB-DNJ than DNJ, which is reversed with maltase (Kato et al., 2005).

The commonalities in substrate specificity suggest similar binding site architectures in hSGLT3 and α-glucosidases. This led us to examine high-resolution crystal structures of α-glucosidases, such as the glycoamylase-DNJ complex (Harris et al., 1993). Primary interactions involve the DNJ C2-, 3-, 4-, and 6-OH groups at contact distances of 2.57 to 3.32 Å from Arg-305, carbonyl-177, Arg-54, and Asp-55, respec-

tively. The nitrogen of DNJ is within 2.82 Å of water molecules 500 and 582. Examination of the free enzyme reveals that DNJ displaces six of seven well ordered water molecules from the binding site, approximately corresponding to the DNJ C2-, 3-, 4-, and 6-OH moieties. These features mirror the interactions of carbohydrates with binding proteins and transporters (Quiocho, 1989; Taroni et al., 2000; Abramson et al., 2003). The essential nature of the C2-, 3-, 4-, and 6-OH groups in the glycoamylase-DNJ complex and in this analysis of hSGLT3 is consistent with a similar substrate binding site.

Primary Sequence Analysis of hSGLT3 and hSGLT1. Significant differences exist between hSGLT3 and hSGLT1 with respect to substrate binding; for example, in hSGLT1: 1) imino sugars do not interact; 2) the C4- or 6-OH moieties are not required for binding; and 3) orientation of the C4-OH is not important (kinetics of glucose $\approx$ galactose). The primary sequences of hSGLT3 and -1 were examined to explain these differences. In the C-terminal sugar binding domain of 9 SGLT1 transporters, 31 polar and aromatic side chains are conserved (Wright et al., 2004, 2006). In hSGLT3, 30 of these 31 residues are conserved; only Glu-457 varying from Gln-457 in hSGLT1. Because studies demonstrated that Gln-457 in hSGLT1 interacts with the pyranose oxygen (Díez-Sampedro et al., 2001), we hypothesized that high-affinity binding of imino sugars to hSGLT3 is due in part to a specific interaction with Glu457. However, a Q457E hSGLT1 mutant does not interact with DNJ (unpublished data), and in the glucoamylase-DNJ complex, the nitrogen of DNJ interacts only with water (Harris et al., 1993). A tertiary structure will probably provide important insights into the high-affinity interaction between imino sugars and hSGLT3.

Glucose and Imino Sugar C4-OH Interaction with hSGLT3 and hSGLT1. The ability of hSGLT3 to discriminate between glucose and galactose (diastereomers at C4) extends to imino sugars, as DGJ $K_{0.5}$/DNJ $K_{0.5}$ = 2750 (Table 1). Substitution of the C4-OH with -F at the equatorial and axial positions did not significantly influence the interaction with hSGLT3, because the kinetics of 4D4Fglc $\approx$ glucose, and neither 4D4Fgal nor galactose interacts with hSGLT3 (Table 1). The ability of -F to mimic the -OH at C4 may be the result

TABLE 1
A summary of the hSGLT3 and hSGLT1 kinetics
Activation parameters $\pm$ S.D. were obtained from 3 to 42 different oocytes.

Substrate	hSGLT3		hSGLT1	
	$K_{0.5}$	$\Delta E_{m(max)}$	$K_{0.5}$	$\Delta E_{m(max)}$
	mM	*% αMDG*	*mM*	*% αMDG*
D-Glucose	19 $\pm$ 6	108 $\pm$ 3	0.5 $\pm$ 0.02[a]	83 $\pm$ 5[a]
αMDG	21 $\pm$ 6	100	0.7 $\pm$ 0.04[a]	100
1DOglc	43 $\pm$ 10	170 $\pm$ 20	10 $\pm$ 1[a]	83 $\pm$ 5[a]
2DOglc	N.D.	N.D.	>100[a]	83 $\pm$ 5[a]
3DOglc	N.D.	N.D.	N.D.	N.D.
4DOglc	> 50 mM	Not Determined	0.4 $\pm$ 0.05	100 $\pm$ 3
4D4Fglc	17 $\pm$ 1	100 $\pm$ 4	0.07 $\pm$ 0.01[a]	83 $\pm$ 5[a]
D-Galactose	N.D.	N.D.	0.6 $\pm$ 0.02[a]	83 $\pm$ 5[a]
4D4Fgal	N.D.	N.D.	1.3 $\pm$ 0.09	110 $\pm$ 2
6-Deoxy-D-glucose	> 50 mM	Not Determined	3 $\pm$ 0.5[a]	83 $\pm$ 5[a]
DNG	0.004 $\pm$ 0.001	260 $\pm$ 36	N.D.	N.D.
DGJ	11 $\pm$ 4	440 $\pm$ 74	N.D.	N.D.
NE-DNJ	0.003 $\pm$ 0.001	130 $\pm$ 36	N.D.	N.D.
NEOH-DNJ (miglitol)	0.003 $\pm$ 0.001	200 $\pm$ 22	N.D.	N.D.
NB-DNJ (miglustat)	0.0005 $\pm$ 0.0001	88 $\pm$ 11	N.D.	N.D.
1SO-DNJ	0.009 $\pm$ 0.004	100 $\pm$ 30	N.D.	N.D.

N.D., not detected; Not Determined indicates the small membrane depolarizations precluded an accurate kinetic assessment.
[a] Data from Diez-Sampedro et al., (2001).

of hydrogen bonding; however, recent evidence suggests organic -F is unlikely to participate in hydrogen bonds (Hoffmann and Rychlewski, 2001; Park et al., 2001; Biffinger et al., 2004; Dunitz, 2004). A possibility is the displacement of water molecules interacting with hSGLT3, which -F would do equally well as -OH. In the unbound state, a hydrated binding site may stabilize hSGLT3 and may need to be disrupted for conformational changes induced by substrate binding to proceed efficiently.

For hSGLT1, less specificity with respect to the C4-OH orientation is observed because the $K_{0.5}$ kinetics of glucose and galactose are approximately equal (Table 1). In addition, the hSGLT1 kinetics for 4DOglc and glucose are approximately equal, suggesting the C4-OH does not contribute significantly. However, an equatorial -F substitution increased the apparent affinity (glucose $K_{0.5}$/4D4Fglc $K_{0.5}$ = 7) for hSGLT1 (Table 1). This may occur through a static dipole-dipole or charge-dipole interaction (Biffinger et al., 2004), for which an -OH group would have relatively less interaction.

Phlorizin Inhibition. This study reveals that phlorizin inhibits hSGLT3, albeit with lower affinity than hSGLT1 (Hirayama et al., 2001). A variation between hSGLT3 and -1 is observed in the potency of phlorizin binding relative to αMDG. For hSGLT1, the αMDG $K_{0.5}$/phlorizin K_i = 2500, whereas in hSGLT3, the αMDG $K_{0.5}$/phlorizin K_i = 175, which exhibts a K_i = 2 ± 0.1 μM. This may arise from structurally different hydrophobic patches (Hirayama et al., 2001) adjacent to the substrate binding site. This assessment is a critical component of establishing a pharmacological profile, providing a concentration range for which phlorizin can discriminate between hSGLT3 and 1.

Variation in Maximum hSGLT3 Responses (Efficacy). An important aspect in identifying pharmacological probes for hSGLT3 is efficacy, the maximal response. For imino sugars, the range of $\Delta E_{m(max)}$ was 88 to 440% of that observed for αMDG. Similar results were obtained for maximum currents recorded under voltage clamp, in that the I_{max} values for DNJ were 290% of those recorded for αMDG in the same hSGLT3 oocyte. N-Alkylation of imino sugars seems to influence this, because the maximum depolarization for NB-DNJ is approximately equal to that of αMDG and, for NE-DNJ, is 2-fold less than for DNJ. The C1-OH also seems to be a factor, in that 1DOglc exhibits a 1.7-fold greater efficacy than αMDG, and substitution at C1 of DNJ results in a reduction of efficacy: 1SO-DNJ $\approx$ αMDG. Finally, the ability of DGJ to induce the largest hSGLT3 response suggests that yet another mechanism, independent of N-alkylation or the C1-OH, influences the maximal response.

Assuming a transporter-like function, the variation in turnover number implies multiple hSGLT3 conformations between agonist binding and membrane depolarization. A similar dependence of turnover number on substrate has been observed with hSGLT1 (Diez-Sampedro et al., 2000). For hSGLT3, this may result from conformational transitions proceeding at different rates depending on the agonist bound, mediated by an induced-fit mechanism (Klingenberg, 2005). For example, the butyl moiety of NB-DNJ may interact with a hydrophobic pocket in hSGLT3 and reduce the rate of a conformational change relative to DNJ. Future experiments modeling hSGLT3, such as concurrent electrophysiology and fluorescent studies (Loo et al., 2005), may help in understanding this variation in efficacy.

Implications of hSGLT3 Activation by Imino Sugars. Clinical trials employing DNJ-based therapeutics may provide important clues regarding hSGLT3 function. Recent clinical trials with NB-DNJ (miglustat) at a target plasma concentration of 10 μM indicate that patients suffered peripheral neuropathies, dose-dependent tremors, paresthesias and cognitive dysfunction (Cox et al., 2000; Pastores and Barnett, 2003; Elstein et al., 2004). Furthermore, in similar clinical trials (Andersson et al., 2004), adverse gastrointestinal effects of NB-DNJ are not observed with the galactose isomer N-butyl-1-deoxygalactonojirimycin. The etiology of these adverse effects is not understood (Pastores and Barnett, 2003).

This study reveals that the concentration of NB-DNJ used in the clinical test (target of 10 μM) is saturating for hSGLT3 ($K_{0.5}$ = 0.5 μM). Because hSGLT3 is expressed at the human neuromuscular junction (Diez-Sampedro et al., 2003), its activation may underlie the peripheral neuropathies and tremors associated with NB-DNJ. Likewise, the hSGLT3 substrate specificity presented here may explain the adverse enteric effects attributable to NB-DNJ but not to N-butyl-1-deoxygalactonojirimycin. This correlation is supported by reports indicating SGLT-mediated glucose sensing (Kim et al., 2001; Gribble et al., 2003; Raybould et al., 2004) and, more specifically, SGLT3-mediated (Freeman et al., 2006) glucose sensing in studies of enteric regulation and nutrient sensing. The substrate specificities identified here, particularly the potent and specific activation by imino sugars will serve as a powerful tool to examine the contribution of hSGLT3 to these adverse effects and explore the physiological role of hSGLT3.

References

Abramson J, Smirnova I, Kasho V, Verner G, Kaback HR, and Iwata S (2003) Structure and mechanism of the lactose permease of *Escherichia coli*. *Science (Wash DC)* **301:**610–615.
Andersson U, Smith D, Jeyakumar M, Butters TD, Borja MC, Dwek RA, and Platt FM (2004) Improved outcome of *N*-butyldeoxygalactonojirimycin-mediated substrate reduction therapy in a mouse model of Sandhoff disease. *Neurobiol Dis* **16:**506–515.
Asano N (2003) Glycosidase inhibitors: update and perspectives on practical use. *Glycobiology* **13:**93R–104R.
Biffinger JC, Kim HW, and DiMagno SG (2004) The polar hydrophobicity of fluorinated compounds. *Chembiochem* **5:**622–627.
Butters TD, Dwek RA, and Platt FM (2005) Imino sugar inhibitors for treating the lysosomal glycosphingolipidoses. *Glycobiology* **10:**43R–52R.
Cox T, Lachmann R, Hollak C, Aerts J, van Weely S, Hrebicek M, Platt F, Butters T, Dwek R, Moyses C, et al. (2000) Novel oral treatment of Gaucher's disease with *N*-butyldeoxynojirimycin (OGT 918) to decrease substrate biosynthesis. *Lancet* **355:**1481–1485.
Diez-Sampedro A, Hirayama BA, Osswald C, Gorboulev V, Baumgarten K, Volk C, Wright EM, and Koepsell H (2003) A glucose sensor hiding in a family of transporters. *Proc Natl Acad Sci USA* **100:**11753–11758.
Diez-Sampedro A, Lostao MP, Wright EM, and Hirayama BA (2000) Glycoside binding and translocation in Na$^+$-dependent glucose cotransporters: comparison of SGLT1 and SGLT3. *J Membr Biol* **176:**111–117.
Diez-Sampedro A, Wright EM, and Hirayama BA (2001) Residue 457 controls sugar binding and transport in the Na$^+$/glucose cotransporter. *J Biol Chem* **276:**49188–49194.
Dunitz JD (2004) Organic fluorine: odd man out. *Chembiochem* **5:**614–621.
Elstein D, Hollak C, Aerts JM, van Weely S, Maas M, Cox TM, Lachmann RH, Hrebicek M, Platt FM, Butters TD, et al. (2004) Sustained therapeutic effects of oral miglustat (Zavesca, *N*-butyldeoxynojirimycin, OGT 918) in type I Gaucher disease. *J Inherit Metab Dis* **27:**757–766.
Freeman SL, Bohan D, Darcel N, and Raybould HE (2006) Luminal glucose sensing in the rat intestine has characteristics of a sodium-glucose cotransporter. *Am J Physiol* **291:**G439–G445.
Godin G, Compain P, Martin OR, Ikeda K, Yu L, and Asano N (2004) Alpha-1-C-alkyl-1-deoxynojirimycin derivatives as potent and selective inhibitors of intestinal isomaltase: remarkable effect of the alkyl chain length on glycosidase inhibitory profile. *Bioorg Med Chem Lett* **14:**5991–5995.
Gribble FM, Williams L, Simpson AK, and Reimann F (2003) A novel glucose-sensing

mechanism contributing to glucagon-like peptide-1 secretion from the GLUTag cell line. *Diabetes* **52:**1147–1154.

Harris EMS, Aleshin AE, Firsov LM, and Honzatko RB (1993) Refined structure for the complex of 1-deoxynojirimycin with glucoamylase from *Aspergillus awamori* var. X100 to 2.4-Å resolution. *Biochemistry* **32:**1618–1626.

Hediger MA, Turk E, and Wright EM (1989) Homology of the human intestinal Na^+/glucose and *Escherichia coli* Na^+/proline cotransporters. *Proc Natl Acad Sci USA* **86:**5748–5752.

Hirayama BA, Diez-Sampedro A, and Wright EM (2001) Common Mechanisms of Inhibition for the Na^+/glucose (HSGLT1) and Na^+/Cl^-/GABA (HGAT1) cotransporters. *Br J Pharmacol* **134:**484–495.

Hoffmann M and Rychlewski J (2001) Effects of substituting a OH group by a F atom in D-glucose. Ab initio and DFT analysis. *J Am Chem Soc* **123:**2308–2316.

Ikeda TS, Hwang ES, Coady MJ, Hirayama BA, Hediger MA, and Wright EM (1989) Characterization of a Na^+/glucose cotransporter cloned from rabbit small intestine. *J Membr Biol* **110:**87–95.

Kato A, Kato N, Kano E, Adachi I, Ikeda K, Yu L, Okamoto T, Banba Y, Ouchi H, Takahata H, et al. (2005) Biological properties of D- and L-1-deoxyazasugars. *J Med Chem* **48:**2036–2044.

Kim M, Cooke HJ, Javed NH, Carey HV, Christofi F, and Raybould HE (2001) D-Glucose releases 5-hydroxytryptamine from human BON cells as a model of enterochromaffin cells. *Gastroenterology* **121:**1400–1406.

Klingenberg M (2005) Ligand-protein interaction in biomembrane carriers. The induced transition fit of transport catalysis. *Biochemistry* **44:**8563–8570.

Loo DD, Hazama A, Supplisson S, Turk E, and Wright EM (1993) Relaxation kinetics of the Na^+/glucose cotransporter. *Proc Natl Acad Sci USA* **90:**5767–5771.

Loo DD, Hirayama BA, Cha A, Bezanilla F, and Wright EM (2005) Perturbation analysis of the voltage-sensitive conformational changes of the Na^+/glucose cotransporter. *J Gen Physiol* **125:**13–36.

Mackenzie B, Loo DD, and Wright EM (1998) Relationships between Na^+/glucose cotransporter (SGLT1) currents and fluxes. *J Membr Biol* **162:**101–106.

Parent L, Supplisson S, Loo DD, and Wright EM (1992a) Electrogenic properties of the cloned Na^+/glucose cotransporter: I. Voltage-clamp studies. *J Membr Biol* **125:**49–62.

Parent L, Supplisson S, Loo DD, and Wright EM (1992b) Electrogenic properties of the cloned Na^+/glucose cotransporter: II. A transport model under nonrapid equilibrium conditions. *J Membr Biol* **125:**63–79.

Park BK, Kitteringham NR, and O'Neill PM (2001) Metabolism of fluorine-containing drugs. *Annu Rev Pharmacol Toxicol* **41:**443–470.

Pastores GM and Barnett NL (2003) Substrate reduction therapy: miglustat as a remedy for symptomatic patients with Gaucher disease type 1. *Exp Opin Investig Drugs* **12:**273–281.

Platt FM and Butters TD (2000) Substrate deprivation: a new therapeutic approach for the glycosphingolipid lysosomal storage diseases. *Expert Rev Mol Med* **2000:**1–17.

Quiocho FA (1989) Protein-carbohydrate interactions—basic molecular-features. *Pure Appl Chem* **61:**1293–1306.

Raybould HE, Cooke HJ, and Christofi FL (2004) Sensory mechanisms: transmitters, modulators and reflexes. *Neurogastroenterol Motil* **16 (Suppl 1):**60–63.

Taroni C, Jones S, and Thornton JM (2000) Analysis and prediction of carbohydrate binding sites. *Protein Eng* **13:**89–98.

van de Laar FA, Lucassen PL, Akkermans RP, Van de Lisdonk EH, Rutten GE, and Van Weel C (2005) Alpha-Glucosidase inhibitors for type 2 diabetes mellitus. *Cochrane Database Syst Rev* CD003639.

Wright EM, Loo DD, Hirayama BA, and Turk E (2004) Surprising versatility of Na^+-glucose cotransporters: SLC5. *Physiology (Bethesda)* **19:**370–376.

Wright EM, Loo DD, Hirayama BA, and Turk E (2006) Sugar absorption, in *Physiology of the Gastrointestinal Tract* (Johnson L, Barrett K, Ghishan F, Merchant J, Said H, and Wood J eds) pp 1653–1665, Elsevier Academic Press, Boston.

Wright EM, van Os CH, and Mircheff AK (1980) Sugar uptake by intestinal basolateral membrane vesicles. *Biochim Biophys Acta* **597:**112–124.

Address correspondence to: Andrew A. Voss, David Geffen School of Medicine at UCLA, Department of Physiology, 10833 Le Conte Avenue, 53-263 Center for Health Sciences, Los Angeles, CA 90095-1751. E-mail avoss@mednet.ucla.edu